Trichostatin A increases SMN expression and survival in a mouse model of spinal muscular atrophy

Amy M. Avila,[1] Barrington G. Burnett,[1] Addis A. Taye,[1] Francesca Gabanella,[2] Melanie A. Knight,[1] Parvana Hartenstein,[1] Ziga Cizman,[1] Nicholas A. Di Prospero,[1] Livio Pellizzoni,[2] Kenneth H. Fischbeck,[1] and Charlotte J. Sumner[1]

[1]Neurogenetics Branch, National Institute of Neurological Disorders and Stroke (NINDS), NIH, Bethesda, Maryland, USA.
[2]Dulbecco Telethon Institute, Institute of Cell Biology (CNR), Rome, Italy.

The inherited motor neuron disease spinal muscular atrophy (SMA) is caused by mutation of the telomeric *survival motor neuron 1* (*SMN1*) gene with retention of the centromeric *SMN2* gene. We sought to establish whether the potent and specific hydroxamic acid class of histone deacetylase (HDAC) inhibitors activates *SMN2* gene expression in vivo and modulates the SMA disease phenotype when delivered after disease onset. Single intraperitoneal doses of 10 mg/kg trichostatin A (TSA) in nontransgenic and SMA model mice resulted in increased levels of acetylated H3 and H4 histones and modest increases in *SMN* gene expression. Repeated daily doses of TSA caused increases in both *SMN2*-derived transcript and SMN protein levels in neural tissues and muscle, which were associated with an improvement in small nuclear ribonucleoprotein (snRNP) assembly. When TSA was delivered daily beginning on P5, after the onset of weight loss and motor deficit, there was improved survival, attenuated weight loss, and enhanced motor behavior. Pathological analysis showed increased myofiber size and number and increased anterior horn cell size. These results indicate that the hydroxamic acid class of HDAC inhibitors activates *SMN2* gene expression in vivo and has an ameliorating effect on the SMA disease phenotype when administered after disease onset.

Introduction

Spinal muscular atrophy (SMA) is an autosomal-recessive motor neuron disease that is the most common inherited disorder lethal to infants (1). Approximately 50% of patients have the most severe form of the disease, type I SMA, with generalized weakness at or soon after birth and death before the age of 2 years without respiratory support (2). Currently, the majority of SMA patients are not diagnosed until after they exhibit muscle weakness, and no therapy is available for this disease.

SMA is caused by homozygous deletions or rare missense mutations in the telomeric copy of the *survival motor neuron 1* (*SMN1*) gene at chromosome 5q13 (3, 4), but all patients retain at least one copy of the centromeric *SMN2* gene. The *SMN1* gene produces full-length SMN mRNA and protein, but the *SMN2* gene predominantly produces mRNA that lacks exon 7 (5, 6) and encodes an unstable protein lacking the last 16 C-terminal residues (7). A minority of *SMN2*-derived transcript is full-length and codes for functional SMN protein. SMA is likely caused by insufficient levels of SMN protein in motor neurons and muscle, with disease severity correlating inversely with *SMN2* gene copy number (8, 9) and SMN expression (10, 11). The SMN protein mediates the assembly of small nuclear ribonucleoproteins (snRNPs), the essential components of the pre-mRNA splicing machinery (12). Cell lines derived from SMA patients show reduced snRNP assembly activity that correlates with reduced SMN protein levels (13), and delivery of snRNPs to zebrafish deficient in SMN ameliorates motor neuron abnormalities (14). These findings suggest that deficiency of snRNP assembly causes SMA; however, SMN may have additional functions in motor neurons (such as in axonal mRNA trafficking) that explain the specific susceptibility of the motor unit to deficiency of this widely expressed protein (15–17).
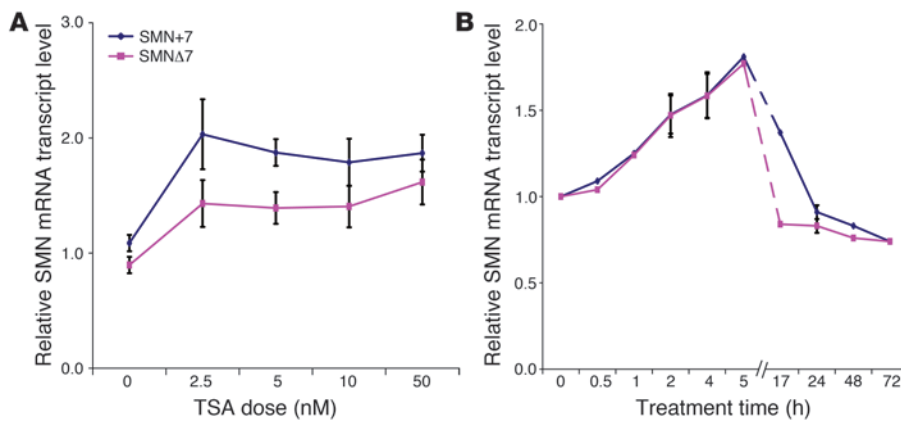
Unlike humans, rodents have a single survival motor neuron gene (*Smn*). Inactivation of this gene leads to very early embryonic death (18). Mice that lack the endogenous *Smn* gene but have 2 copies of a transgenic human *SMN2* gene develop a type I SMA phenotype, with a median survival of approximately 6 days (19). SMA mice that also possess an additional transgene expressing high levels of SMN transcript lacking exon 7 have a median survival of approximately 2 weeks, indicating that truncated SMN protein can be partially functional (20). Importantly, mice that express 8–16 copies of the *SMN2* gene are completely rescued from the disease phenotype, recapitulating the dose relationship between *SMN2* copy number and disease severity observed in humans and indicating that a sufficient level of *SMN2* gene product can in itself prevent the disease (19).

Because all SMA patients have at least one copy of the *SMN2* gene, increasing SMN expression has emerged as one of the most promising SMA treatment strategies. Cell-based, high-throughput compound screens have been completed and are intended to identify compounds that increase SMN levels by activating the *SMN2* promoter, increasing exon 7 inclusion in *SMN2*-derived transcripts, or stabilizing SMN protein levels (21, 22). Histone deacetylase (HDAC) inhibitors can increase expression of genes by modifying chromatin structure (23). These drugs — which include

Figure 1
TSA activates the *SMN2* gene in vitro. (**A**) The SMA fibroblast cell line 2906 was treated with 0–50 nM TSA, and SMN+7 and SMNΔ7 mRNA was measured after 4 hours. Values represent mean ± SEM of 5 separate experiments. (**B**) The SMA fibroblast cell line 3813 was treated with 50 nM TSA, and SMN+7 and SMNΔ7 mRNA levels were determined over a period of 0–72 hours. Values represent mean ± SEM of 2 experiments for the 2-, 4-, 17-, and 24-hour time points and 1 experiment for the 0.5-, 1-, 5-, 48-, and 72-hour time points.

at least 4 biochemical classes (aliphatic acids, hydroxamic acids, benzamides, and cyclic peptides) — have been actively developed for the treatment of hematological disease and malignancy. We have previously demonstrated that HDAC inhibitors from different biochemical classes are able to activate the *SMN2* promoter through direct modification of the acetylation state of histones at the promoter (24). The aliphatic acids valproic acid (VPA), sodium butyrate, and phenylbutyrate (PBA) (25–28) increase full-length SMN mRNA and protein in cell lines derived from SMA patients, in part by activating the *SMN2* promoter and in part by promoting exon 7 inclusion in SMN transcript via increased expression of the SR protein Htraβ1 (26). Sodium butyrate has also been shown to improve the survival of SMA pups when administered to pregnant mothers (27). These results have prompted early clinical trials with VPA and PBA in SMA patients (29, 30). These 2 drugs were readily available for patient trials because they are in widespread clinical use, but they are weak HDAC inhibitors and have multiple other off-target biological effects that may minimize their effectiveness. The newer, more potent HDAC inhibitors may be more effective for the treatment of SMA, but to date the fundamental preclinical proof of concept that these compounds can increase SMN levels in vivo has been lacking. Also lacking is proof that HDAC inhibition per se can be effective after disease onset. Here we show that the highly specific and potent HDAC inhibitor trichostatin A (TSA) caused increased SMN levels, improved motor unit pathology, and improved motor function and survival in a mouse model of SMA treated after disease onset. These studies provide a strong rationale to develop newer, more potent HDAC inhibitors for the treatment of SMA and to evaluate the efficacy of these compounds in SMA patients.

Results

TSA activates SMN2 gene expression in vitro. TSA was previously shown to increase activation of an *SMN2* promoter reporter by approximately 2-fold with an EC_{50} of 17 nM in a transgenic motor neuronal cell line (21). In order to confirm activation of the endogenous human *SMN2* gene in vitro, a fibroblast cell line derived from a type III SMA patient (cell line no. 2906; see Methods) was treated for 4 hours with a range of doses of TSA (2.5–50 nM). All TSA doses tested led to increased mRNA levels of SMN containing exon 7 (SMN+7) and SMN lacking exon 7 (SMNΔ7) above vehicle-treated levels (Figure 1A). In this cell line, SMN+7 mRNA levels increased to a greater degree than did SMNΔ7 mRNA levels. This may indicate that TSA has dual effects, activation of the *SMN2* promoter and promotion of exon 7 inclusion in SMN transcripts, as has been described for other HDAC inhibitors and SMN (25, 26). A fibroblast cell line derived from a type I SMA patient (cell line no. 232; see Methods) was also treated for 4 hours with a larger range of TSA doses (0.05–100 nM). These experiments showed a dose-dependent increase in both SMN+7 and SMNΔ7 mRNA levels, with a maximum induction of 1.7-fold at 50 nM (data not shown). A third fibroblast cell line derived from another type I SMA patient (cell line no. 3813; see Methods) was treated for various time periods with 50 nM TSA. Again, an approximately 2-fold increase over baseline in SMN+7 and SMNΔ7 mRNA levels was observed. This effect was rapid in onset and transient, with increased levels evident at 1 hour and a return to baseline by 24 hours (Figure 1B). The increase in SMNΔ7 mRNA appeared to be shorter lived than that of SMN+7 mRNA, which may indicate that the SMNΔ7 mRNA species is more unstable.

A single dose of TSA increases histone acetylation and SMN gene expression in mice. In order to determine what dose of TSA inhibits HDACs and modifies gene expression in different tissue compartments, nontransgenic mice were treated with single intraperitoneal doses of 2, 5, or 10 mg/kg TSA, doses that have previously been used in mice (31–33). Liver and brain tissues were isolated after 2 hours. Dose-dependent increases in acetylated H3 and H4 histones were evident in both brain and liver, with an approximately 15-fold induction in the brain (Figure 2, A and B). Quantitative RT-PCR (qRT-PCR) was used to measure the mRNA levels of mouse SMN and follistatin. Follistatin, which interacts with members of the TGF-β family, was measured as a positive control because it has been previously shown to be activated by TSA (34). We observed increases in follistatin mRNA in both brain and liver and an increase of mouse SMN mRNA in liver (Figure 2C). Because the 10-mg/kg TSA dose produced the greatest increase in acetylated histone levels and in gene expression, this dose was used for all subsequent experiments.

TSA has been previously shown to have rapid pharmacokinetics in the mouse: mice dosed by intraperitoneal injection had absorption into the plasma within 2 minutes and a plasma $t_{1/2}$ of approximately 5–10 minutes (31). In order to investigate the time course of gene activation by TSA, nontransgenic mice were treated with single doses of 10 mg/kg TSA, and tissues were harvested at 2, 4, 6, and 16 hours after dosing. These studies revealed maximal gene activation at approximately 2–4 hours, with a return to base-
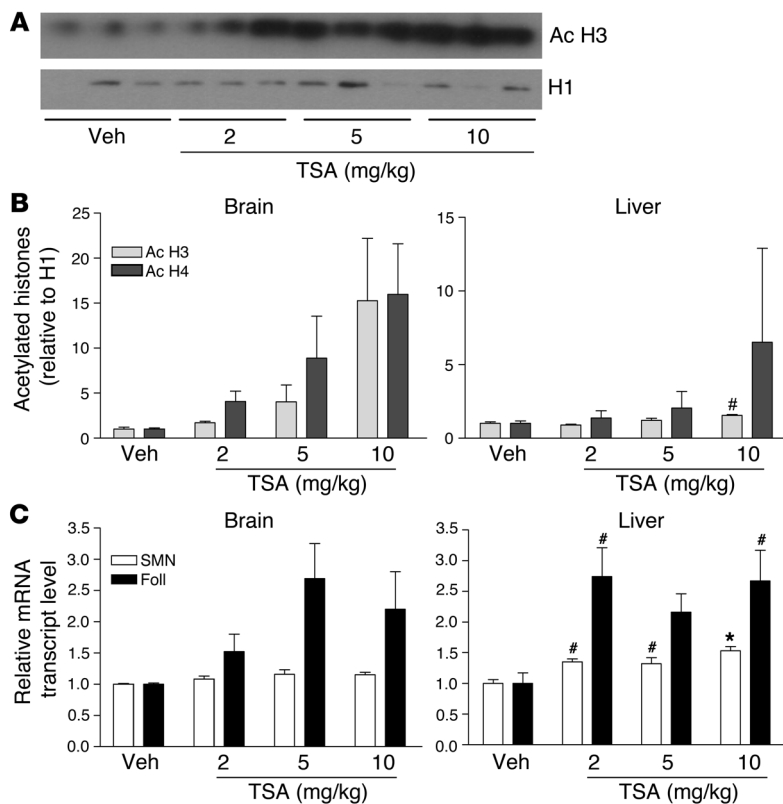
Figure 2
TSA treatment increases histone acetylation and gene expression in nontransgenic mice. (**A**) Representative Western blot showing acetylated H3 (Ac H3) histones compared with H1 histone levels in the brains of nontransgenic mice 2 hours after treatment with vehicle (Veh) or with 2, 5, or 10 mg/kg TSA. Each lane represents an individual animal. (**B**) Quantification of acetylated H3 and H4 histones in the brains and livers of nontransgenic mice treated with vehicle or with 2, 5, or 10 mg/kg TSA. (**C**) Mouse Smn and follistatin (Foll) mRNA levels after treatment with vehicle or with 2, 5, or 10 mg/kg TSA. Values represent mean ± SEM of 3 mice per group. *$P < 0.01$; #$P < 0.05$.

line by 16 hours (Supplemental Figure 1; supplemental material available online with this article; doi:10.1172/JCI29562DS1). No changes in SMN protein levels were observed at any time point (data not shown). The 2- or 4-hour time points were selected for all subsequent experiments.

We next treated a cohort of nontransgenic mice with a single dose of 10 mg/kg TSA ($n = 8$) or vehicle ($n = 7$), and brain, liver, spinal, and muscle tissues were harvested at 2 hours for determination of mRNA and protein levels. Follistatin mRNA increased in brain and liver, as expected, but did not change in spinal cord and muscle tissues (Figure 3A). This result in muscle was consistent with previous observations that follistatin is not induced in healthy muscle, only in injured muscle (34). In order to verify that TSA was modulating gene expression in these tissues, qRT-PCR was performed for brain-derived neurotrophic factor (BDNF), another gene that has been shown to be activated by HDAC inhibitors (35). Increases in BDNF mRNA were evident in spinal cord and muscle, verifying the biological effect of TSA in these tissues (Figure 3A). TSA treatment also resulted in a modest, but significant, increase in mouse SMN mRNA in the liver ($P < 0.001$) and muscle ($P < 0.05$; Figure 3A). No change in SMN or BDNF protein expression was found in these tissues (Figure 3B).

In order to verify the HDAC-inhibitory effects of TSA in SMA model mice, P10 SMA mice ($Smn^{-/-}SMN2^{+/+}SMN\Delta7^{+/+}$; ref. 20) were treated with a single dose of 10 mg/kg TSA or vehicle, and brain and liver tissues were harvested at 2 hours. Acetylated H3 and H4 levels increased in the brain and to a lesser extent in the liver (Supplemental Figure 2). A cohort of P10 SMA mice was next treated with a single dose of 10 mg/kg TSA or vehicle ($n = 7$ per group), and liver, brain, spinal cord, and muscle tissues were harvested after 4 hours. No changes in SMN+7 mRNA were observed, and

small increases in SMNΔ7 mRNA were seen in all tissues (data not shown). No changes in SMN protein levels were observed in any of these tissues (data not shown). Together, these results indicate that single doses of TSA cause dose-dependent and time-limited inhibition of HDACs and a modest increase in *SMN* gene expression, but no change in SMN protein expression.

Repeated doses of TSA increase SMN2 gene expression, SMN protein levels, and snRNP assembly activity in SMA mice. Given the lack of change in SMN protein levels after a single dose of TSA, we postulated that multiple doses might be required. Consequently, we treated a cohort of mice beginning on P5 with daily injections of TSA 10 mg/kg and harvested tissues 4 hours after the last dose on P13 (Figure 4). As expected based on the single-dosing experiments in nontransgenic mice, BDNF mRNA increased approximately 2-fold in spinal cord and muscle (Figure 4A). Follistatin no longer served as a good marker of gene activation in brain and liver in chronically treated mice, as levels of this mRNA either did not change or decreased, suggesting that this gene may be autoregulated and become silenced with chronic stimulation. Follistatin levels significantly decreased in SMA mouse muscle, in contrast to a recently reported increase of follistatin in mouse muscular dystrophy models (36). SMN+7 mRNA levels increased in the brain, liver, and spinal cord, although these changes did not reach statistical significance, whereas SMN+7 levels increased approximately 5-fold ($P < 0.01$), and SMNΔ7 levels increased approximately 2-fold ($P < 0.01$), in muscle. Western blot analysis of protein isolated from these tissues revealed the presence of both the full-length SMN protein and the SMNΔ7 protein, as has been previously described in these mice (20). Full-length SMN and SMNΔ7 protein levels increased by approximately 1.5- to 2-fold in the brain, liver, and spinal cord with TSA treatment (Figure 4B). This increase was apparent for both SMN isoforms. No obvious
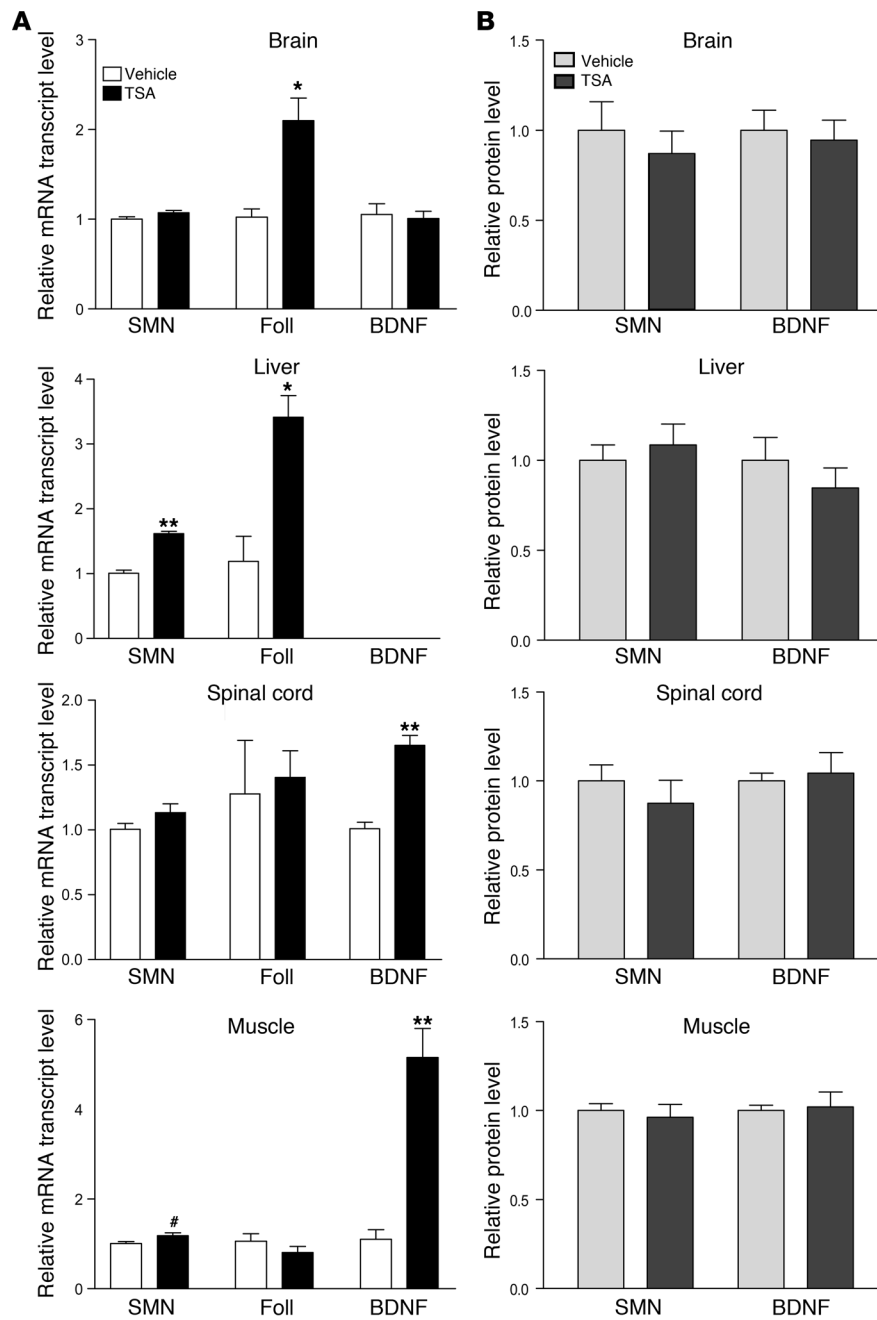
A

B

Figure 3
A single dose of TSA increases *Smn* gene expression but not SMN protein levels in nontransgenic mice. (**A**) Smn, follistatin, and BDNF mRNA levels and (**B**) SMN and BDNF protein levels were determined in brains, livers, spinal cords, and muscle tissues 2 hours after nontransgenic mice were treated with a single dose of TSA (10 mg/kg; $n = 8$) or vehicle ($n = 7$). BDNF mRNA levels were too low in liver to be reliably measured. Values represent mean ± SEM. $^\#P < 0.05$; $^*P < 0.01$; $^{**}P < 0.001$.

rate assembly of Sm proteins and snRNAs into snRNPs (12). In order to investigate the activity of the SMN complex in vehicle- and TSA-treated SMA mice and heterozygous littermates, snRNP assembly activity was measured in brain extracts prepared from P13 mice using a previously described in vitro assay (37). Only brain tissues could be analyzed at this time point because of the strong physiological downregulation of SMN activity that occurs postnatally in several tissues, including the spinal cord (38). Western blot analysis of the prepared extracts confirmed an increase in SMN protein levels similar to those demonstrated in Figure 4B (data not shown). In vitro, transcribed radioactive U1 snRNAs were incubated with the extracts, anti-Sm antibodies were used to immunoprecipitate assembled snRNPs, and U1 snRNA levels were quantified to determine the relative snRNP assembly efficiency. Heterozygous vehicle-treated mice showed approximately 5-fold greater snRNP assembly activity than did vehicle-treated SMA mice (data not shown). A detailed analysis of the impairment of SMN activity in snRNP assembly in mouse models of SMA will be reported elsewhere (F. Gabanella, M.E.R. Butchbach, A.H. Burghes, and L. Pellizzoni, unpublished observations). TSA treatment improved snRNP assembly activity by approximately 1.8-fold ($P < 0.0017$), comparable to the improve-

change in the ratio of full-length to SMNΔ7 protein was evident. Western blot of muscle tissues showed that SMN protein bands were very faint or undetectable in vehicle-treated samples but were visible in the TSA-treated mice, indicating an increase (Figure 4B). Despite increases in BDNF mRNA, mature BDNF protein as measured by ELISA showed no change in response to TSA treatment (Figure 4C). No differences in SMN mRNA or protein levels were observed between TSA and vehicle-treated heterozygous littermate mice (data not shown).

Spliceosomal snRNPs are composed of 1 small nuclear RNA (snRNA) molecule, a common core of 7 Sm proteins, and additional proteins specific for each snRNP. To date, the best characterized function of the SMN complex is to mediate the efficient and accu-

ment in SMN protein levels (Figure 5, A and B). In contrast, no differences in snRNP assembly were observed in brain extracts derived from vehicle- and TSA-treated heterozygous littermates (Supplemental Figure 3). These data indicate that increased SMN protein levels are associated with increased SMN activity in snRNP assembly in brain extracts of TSA-treated SMA mice.

TSA treatment improves survival of SMA mice when started after disease onset. Having observed that repeated daily doses of TSA increased SMN protein levels and snRNP assembly activity, we next examined whether TSA treatment ameliorates the disease phenotype in SMA mice. The $Smn^{-/-}SMN2^{+/+}SMN\Delta7^{+/+}$ SMA mice have been reported to have severe muscle weakness, approximately 20% loss of anterior horn cells (AHCs), diffusely small myofibers, and a median
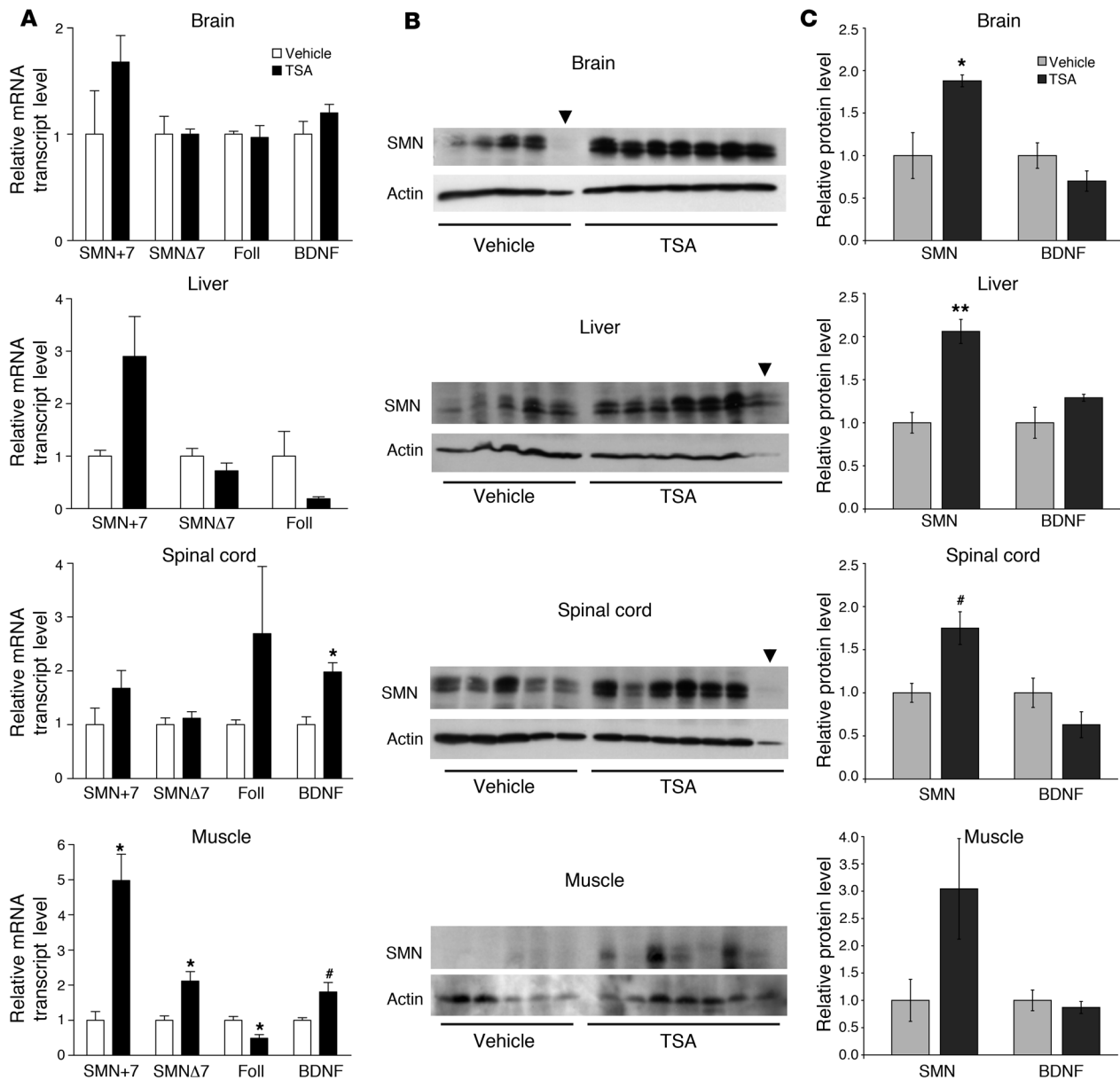
Figure 4
Repeated doses of TSA increase SMN+7 mRNA levels and SMN protein levels in SMA mice. (**A**) SMN+7, SMNΔ7, follistatin, and BDNF mRNA levels and (**B** and **C**) SMN and BDNF protein levels were determined in brain, liver, spinal cord, and muscle isolated 4 hours after the last dose from SMA mice treated daily from P5 through P13. (**B**) Western blots, with each lane representing 1 animal. In the upper panels, the upper bands show full-length SMN protein; the lower bands show SMNΔ7 protein. (**C**) Quantification of Western blots shown in **B**. Lanes denoted with arrowheads were excluded as underloaded relative to the other visualized lanes. SMN protein bands were not visible in the muscle of untreated SMA mice, although they were evident in treated mice; therefore, quantification of the changes in muscle SMN protein levels was limited. Values represent mean ± SEM. $^{\#}P < 0.05$; $^{*}P < 0.01$; $^{**}P < 0.001$.

survival of approximately 2 weeks (20). In addition, by P5 the mice show clear manifestations of disease: they are significantly underweight and have a markedly impaired righting reflex (20). In order to test whether HDAC inhibitors are beneficial when delivered after disease onset, we administered once-daily injections starting at P5 and continued until P20. All the pups in litters derived from heterozygous *Smn*^{+/−}*SMN2*^{+/+}*SMNΔ7*[+/+] breeding pairs (including 48 SMA, 101 heterozygous, and 60 WT littermates (Figure 6A) were randomly assigned to receive TSA or vehicle, and pups were

monitored daily by recording weight and performing behavioral tests. Of the heterozygous and WT littermates, 5 TSA-treated and 3 vehicle-treated mice died during the treatment period, most of them presumably from injection injury. As expected, before the start of treatment P5 SMA mice were significantly underweight (2.85 ± 0.09 g versus 3.32 ± 0.06 g; $P < 0.0001$) and had significantly impaired righting time (24.9 ± 1.5 s versus 5.1 ± 0.7 s; $P < 0.0001$) compared with WT and heterozygous littermates. The cohorts of SMA mice receiving TSA or vehicle were equally matched for weight
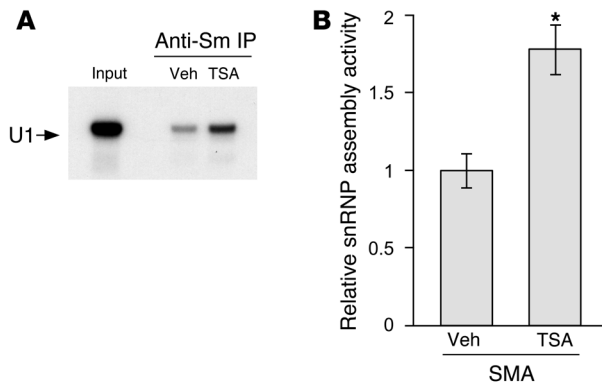
Figure 5
TSA treatment increases snRNP assembly activity in brains of SMA mice. (**A**) snRNP assembly reactions were carried out using in vitro transcribed radioactive U1 snRNA and 25 mg of brain extracts from either vehicle- or TSA-treated SMA mice. Following immunoprecipitation with anti-Sm antibodies, input (2.5%) and immunoprecipitated U1 snRNAs were analyzed by electrophoresis on 10% polyacrylamide, 8M urea denaturing gels and autoradiography. (**B**) Quantification of relative snRNP assembly activity in brain extracts from vehicle- and TSA-treated SMA mice. Brain extracts from either vehicle-treated ($n = 5$) or TSA-treated ($n = 7$) SMA mice were prepared and analyzed by snRNP assembly and immunoprecipitation experiments as in **A**, and the amount of immunoprecipitated U1 snRNA was quantified as described in Methods. Values represent mean ± SEM. *$P < 0.01$.

(2.82 ± 0.12 g versus 2.87 ± 0.14 g) and litter size (8.1 ± 0.4 versus 8.2 ± 0.5) at P5. Of the 48 SMA mice treated with TSA, 3 pups were lost during cage maintenance and were therefore excluded from the survival analysis. TSA-treated SMA mice showed significantly improved survival compared with vehicle-treated mice ($P = 0.0003$, log-rank test; Figure 6B). The median difference in survival was 3 days, or 19% (19 versus 16 days), with one-quarter of the mice showing no improvement in survival and one-quarter of the mice showing an improvement of 30% or better. The pups with increased survival of 30% or greater tended to have less weight loss compared with WT and heterozygous littermates at P5 (0.35 ± 0.12 g versus 0.55 ± 0.22 g) and smaller litter size (7.3 ± 0.9 versus 8.8 ± 0.1), although these differences did not reach statistical significance. No statistically significant difference in survival between male and female mice was observed (data not shown).

SMA mice treated with TSA also showed an increased maximal weight and reduced weight loss compared with vehicle-treated mice that was evident starting at P13 ($P = 0.02$; Figure 6C). This occurred

even though TSA caused some decrease in weight gain in the treated WT and heterozygous littermates (Figure 6C). Mice treated with TSA were observed to have some diarrhea. This was further investigated with blood chemistry and hematology panels and gross and microscopic examinations at necropsy of 5 TSA-treated and 2 vehicle-treated WT and heterozygous littermates. These studies showed no abnormalities (data not shown). After termination of drug treatment, the weight difference between TSA- and vehicle-treated WT and heterozygous mice decreased by P30 (18.93 ± 0.66 g versus 19.53 ± 0.71 g) and was no longer apparent at P60 (23.64 ± 0.67 g versus 23.29 ± 0.73 g). SMA mice also showed improved motor function, as assessed by timed righting (Figure 6D). Improvement in righting was evident starting at P9 ($P = 0.03$), well before the attenuation of weight loss became apparent at P13. TSA-treated mice also showed improved ambulation (Supplemental Video) as well as improved forelimb grip strength (Supplemental Figure 3).

TSA improves the morphology of the motor unit. In order to investigate the pathological correlate of this amelioration in the SMA dis-

Figure 6
TSA increases survival, attenuates weight loss, and enhances motor behavior of SMA mice. SMA mice and their WT and heterozygous littermates were treated with daily intraperitoneal injections of TSA (10 mg/kg) or vehicle on days P5–P20. (**A**) Four mice from the same litter at P13, showing the gross appearance of a TSA-treated SMA mouse, a vehicle-treated SMA mouse, a heterozygous (Het) mouse, and a WT mouse. (**B**) Kaplan-Meier survival curves of mice treated with TSA ($n = 23$) or vehicle ($n = 22$). $P < 0.0003$, log-rank test. (**C**) Weights of SMA mice treated with TSA ($n = 26$) or vehicle ($n = 22$), heterozygous mice treated with TSA ($n = 52$) or vehicle ($n = 49$), and WT mice treated with TSA ($n = 30$) or vehicle ($n = 30$). (**D**) Righting time in SMA mice treated with TSA ($n = 20$) or vehicle ($n = 15$), heterozygous mice treated with TSA ($n = 29$) or vehicle ($n = 37$), and WT mice treated with TSA ($n = 12$) or vehicle ($n = 19$).
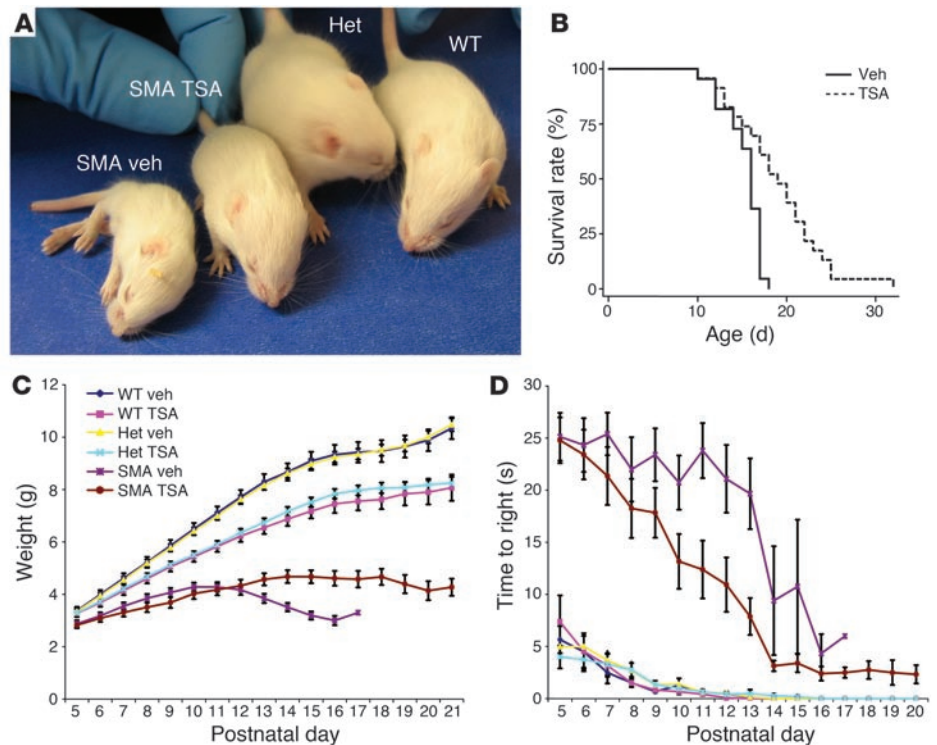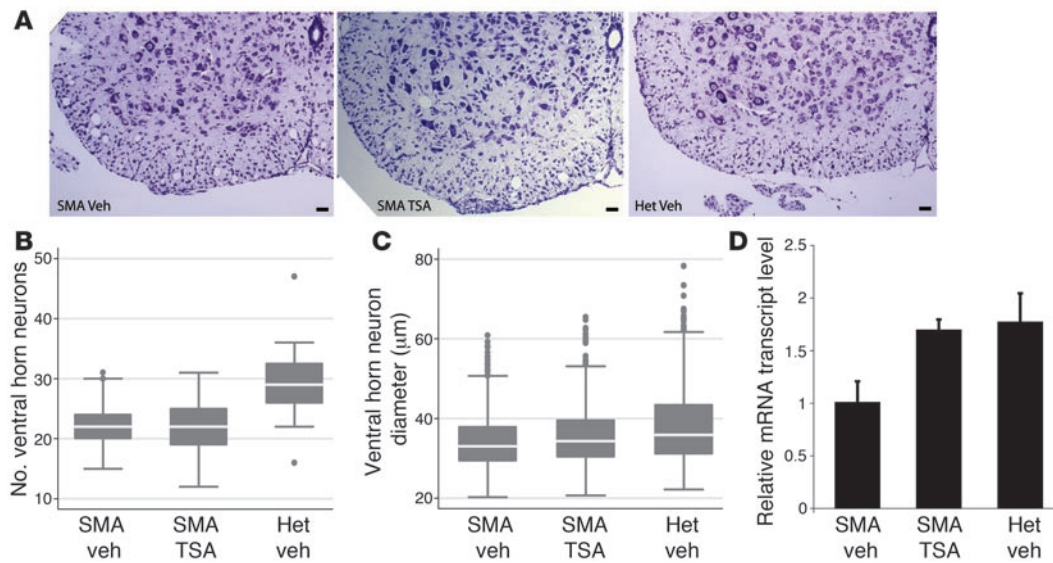
Figure 7
TSA increases AHC size but not AHC number. SMA mice were treated with vehicle (*n* = 3) or TSA (*n* = 3) and heterozygous littermates were treated with vehicle (*n* = 3) on days P5–P13. (**A**) Nissl-stained cross-sections of lumbar spinal cord showing 1 ventral horn. Scale bars: 10 μm. (**B**) Median ventral horn neuron number was reduced in SMA mice compared with heterozygous littermates (*P* < 0.0001) and was not changed by TSA treatment. Lines represent median values, boxes represents the twenty-fifth and seventy-fifth percentiles, whiskers represent values within 1.5 times the interquartile range, and dots represent outliers. (**C**) Median ventral horn neuron size was increased in heterozygous mice compared with SMA mice (*P* < 0.0001) and was increased by TSA treatment (*P* = 0.003). (**D**) ChAT mRNA levels were determined in spinal cord isolated from SMA mice treated daily with vehicle (*n* = 5) or TSA (*n* = 5) and heterozygous littermates treated with vehicle (*n* = 6) on days P5–P13.

ease phenotype, we treated a cohort of mice (4 SMA vehicle-treated mice, 4 SMA TSA-treated mice, and 3 vehicle-treated heterozygous littermates) beginning on P5 and sacrificed them on P13 for examination of muscle and spinal cord tissues. The weight of one of the mice in the vehicle-treated SMA group was nearly 3 standard deviations above the mean weight of P13 vehicle-treated SMA mice in the survival analysis, perhaps because this mouse was derived from an unusually small litter of only 2 pups. We considered this mouse an outlier, and the pathological data was analyzed both including and excluding this mouse.

We analyzed the diameter and number of neurons greater than 25 μm in the ventral horn of the lumbar spinal cord at 15 levels. The median number of ventral horn neurons per level in heterozygous mice was 29, compared with 22 in both SMA vehicle-treated and SMA TSA-treated mice (Figure 7, A and B). These neurons had a median diameter of 35.9 μm in heterozygous littermates, 33.0 μm in vehicle-treated SMA mice, and 34.3 μm in TSA-treated SMA mice (Figure 7, A and C). These data show that SMA caused some decrease in AHC number and size and that TSA treatment increased AHC size (*P* = 0.003), but not AHC number. This difference in AHC size between and vehicle- and TSA-treated SMA mice diminished (34.0 μm versus 34.3 μm) and was no longer statistically significant with inclusion of the outlier mouse (*P* = 0.16). We next measured the mRNA levels of the acetylcholine synthesis enzyme choline acetyltransferase (ChAT) as alterations of this marker have been described in different experimental conditions associated with axonal damage (39, 40). Vehicle-treated SMA mouse spinal cords showed reduced ChAT expression compared with heterozygous littermates, whereas TSA treatment resulted in increased ChAT levels in SMA mouse spinal cords (Figure 7D).

The main pathological abnormality of SMA mouse muscles compared with normal heterozygous littermates was globally small myofibers. These fibers had a small cytoplasm without a change in the number of nuclei per fiber. There was no evidence of fibrosis, inflammatory infiltrate, or abundant degeneration. Only very rare fibers showed centralized nuclei, the hallmark feature of regenerating myofibers. The median total cross-sectional area, diameter of myofibers, and number of myofibers in the tibialis anterior (TA) muscle were significantly reduced in SMA mice compared with heterozygous littermates (Figure 8, A–E). TSA treatment resulted in a statistically significant improvement in total muscle area (*P* = 0.03) and median myofiber diameter (*P* < 0.0001; Figure 8, A–D) and a trend toward improvement in median myofiber number (*P* = 0.08) when the outlier mouse was excluded (Figure 8E). With the outlier included, the increase in myofiber diameter was still statistically significant (*P* < 0.0001), but the increases in total cross-sectional area and total myofiber number were no longer significant (*P* = 0.25 and *P* = 0.39, respectively). TSA treatment resulted in no change in the number of nuclei per myofiber, nor did it cause an increase in the number of myofibers with centralized nuclei (data not shown), indicating that there were no histological features of regeneration.

In order to further explore the mechanism of improvement in the neuromuscular pathology, we next analyzed the expression pattern of markers associated with muscle regeneration and differentiation. Postnatal myofiber size is determined by 2 distinct mechanisms: (a) regulation of cytoplasmic volume associated with individual myonuclei, a process dependant on rates of protein synthesis and degradation (41), and (b) control of the number of myonuclei within an individual myofiber, a process involving fusion of activated satellite cells with existing
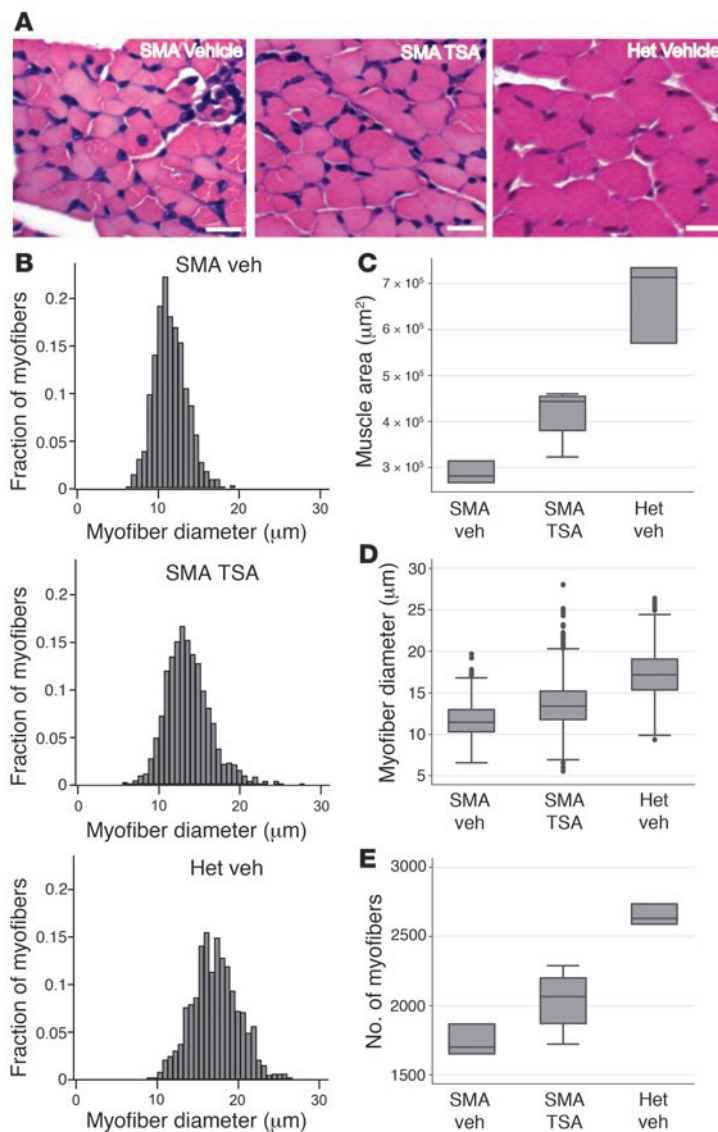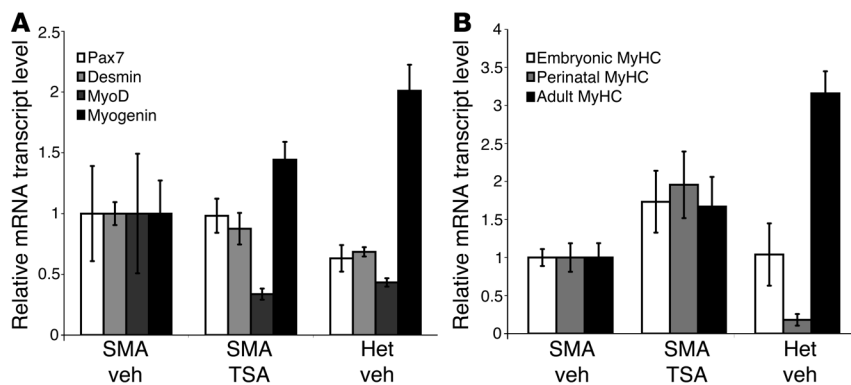
Discussion

The devastating neuromuscular disease SMA is caused by reduced expression of full-length SMN mRNA and protein. Developing methods to increase SMN levels in SMA patients is currently the most actively pursued therapeutic strategy. We and others have shown that HDAC inhibitors activate SMN expression in vitro (25–28). Here we demonstrated that the potent and selective HDAC inhibitor TSA significantly improved motor performance, attenuated weight loss, increased survival, and improved the pathology of the motor unit in SMA model mice. Our results provide a strong preclinical basis for examining the newer, more potent HDAC inhibitors in clinical trials in SMA patients.

The neuromuscular pathology of severe SMA has long been recognized as distinct from other motor neuron diseases. Autopsy studies on type I SMA patients have documented loss of large-diameter AHCs in the spinal cord; however, the muscle shows seas of rounded, small myofibers rather than angulated, grouped myofibers typical of denervation (45). These myofibers appear to be arrested ultrastructurally in development (43) and express abnormally increased amounts of developmental isoforms of myosin (44). Such observations have raised the idea that SMA is not a cell-autonomous disease and that SMN deficiency may result in primary abnormalities in both motor neuron and muscle compartments that lead to a failure of trophic support between the presynaptic and postsynaptic components of the neuromuscular synapse. Loss of the motor neuron cell body may be a late event that follows longstanding dysfunction at the nerve terminus and motor end plate. Evidence from several in vitro and animal studies supports this hypothesis. Primary motor neurons isolated from SMA mice have been shown to have morphological abnormalities of distal termini with shortened axonal length and small growth cones (17), while SMA patient–derived myoblasts and Smn-deficient C2C12 myoblasts show impairment of myofiber proliferation and fusion (46, 47). Coculture of satellite cells derived from SMA patients with motor neurons causes premature motor neuron disorganization and death, suggesting a failure of trophic support by SMA muscle for motor nerves (48). *Drosophila* deficient in SMN show both pre-and postsynaptic disorganization of the neuromuscular junction, and replacement of SMN is required in both the motor neuron and muscle compartments in

fibers or with themselves to form a new myofiber (42). Compared with heterozygous mouse muscle, vehicle-treated SMA mouse muscle showed slightly increased expression of Pax7, desmin, and MyoD, markers associated with early satellite cell activation, and reduced expression of myogenin, a marker of terminal differentiation of muscle cells (Figure 9A). In addition, vehicle-treated SMA mice showed increased expression of perinatal myosin heavy chain (MyHC) and reduced expression of adult MyHC compared with heterozygous littermates (Figure 9B). Together these results indicate immaturity of SMA muscle, as has been described in previous ultrastructural and biochemical studies (43, 44). TSA treatment of SMA mice did not result in an increase in early satellite cell activation markers, but did result in increased expression of myogenin and all of the MyHC isoforms. These results, together with our histological findings, suggest that the increased size of myofibers in TSA-treated SMA mice is caused by enhanced synthesis of contractile filaments and increased maturity of muscle cells rather than by activation of new satellite cells and regeneration.

Figure 9
TSA increases maturity of SMA myofibers. (**A**) Pax7, desmin, MyoD, and myogenin and (**B**) embryonic, perinatal, and adult MyHC mRNA levels were determined in muscle isolated from SMA mice treated daily with vehicle ($n = 5$) or TSA ($n = 6$) and heterozygous littermates treated with vehicle ($n = 5$) on days P5–P13. Values represent mean ± SEM.

this model to provide rescue (49). In our study in mice at near–end stage, we observed a marked and homogeneous decrease in the size of myofibers as well as a reduction in the number of myofibers, associated with a less striking 24% decrease in AHC number in SMA mice compared with heterozygous littermates. The decreased size of the remaining AHCs and the global abnormality of myofibers imply dysfunction — without cell death — of the remaining motor units in SMA mice. TSA treatment improved the pathology of the muscle, but also caused an increase in AHC size and in ChAT expression, indicating improved function of the entire motor unit. This interpretation is supported by previous data documenting that the size of the motor neuron cell body correlates with the size of the motor unit during recovery after denervation injury (50).

Because skeletal muscle is a source of signals that influence motor neuronal survival, growth, and maintenance (51), it is possible that TSA exerts its primary effect on SMA muscle, with indirect benefits to AHCs. Recently, HDAC inhibitors have been shown to activate satellite cells and myofiber regeneration via induction of follistatin (34), and in so doing improve the pathology and function of mice with muscular dystrophy (36). Although it is possible that follistatin induction plays a role in the recovery of SMA mice during TSA treatment, we believe this is unlikely. We observed no induction of follistatin in any of the cohorts of nontransgenic or SMA mice treated with TSA; rather, follistatin was significantly decreased in the muscle of repeatedly dosed SMA mice. This is not surprising, as it has been previously observed that follistatin induction occurs only in the context of injured muscle, not healthy muscle, and relates to the capacity for robust satellite cell activation and muscle regeneration (34). In our study, SMA mouse muscle did not show the hallmark pathological feature of muscle regeneration, centrally nucleated fibers, before or after TSA treatment. Furthermore, TSA-treated SMA mice showed no increase in expression of markers associated with early satellite cell activation, i.e., Pax7 or MyoD. Rather, TSA treatment caused increased expression of myogenin, a marker of terminal muscle cell differentiation. This was associated with improved expression of all the myosin isoforms and increased size of myofibers, suggesting increased synthesis of contractile proteins in individual myofibers. These data indicate that the principal effect of TSA in SMA is not to promote muscle regeneration, but rather to improve the maturation of existing myofibers, prevent myofiber degeneration, and improve the health of the entire motor unit.

The central biochemical defect in SMA is a deficiency of full-length SMN mRNA and protein. In this study, we have demonstrated that treatment with the HDAC inhibitor TSA activates *SMN* gene expression and, after repeated doses, increases SMN protein levels in neural and muscle tissues in SMA mice. These data represent an important confirmation that the HDAC-inhibitory effects observed in vitro can also occur in vivo. We observed a range of *SMN* gene activation in different tissues, with muscle showing the most robust increase in full-length SMN transcript in SMA mice. Muscle was also the tissue with the lowest levels of baseline SMN expression at the P13 time point. Differences in *SMN* gene activation likely related to differences in the specific complex of proteins, including HDACs, histone acetyltransferases, and transcription factors that regulate SMN in specific cell types (52). We have previously shown that HDAC2 likely plays an important role in repressing SMN gene expression during development (24), and it may be that the concentrations of this HDAC and others regulating SMN gene expression are higher in muscle. In addition to showing an increase in the total cellular SMN protein level, we also showed that this increase resulted in an improvement of snRNP assembly activity in brain extracts. This indicates that the induced SMN protein is incorporated into the SMN complex and performs its normal function in snRNP biogenesis. Because snRNP assembly activity is too low to measure at the P13 time point in muscle and spinal cord, we were unable to confirm that the increases in SMN protein observed in these tissues also corresponded to improved snRNP assembly. This is very likely, however, in the context of data showing that snRNP activity correlates with total SMN protein levels in vitro and in vivo (13) (L. Pellizzoni, unpublished observations).

The improvements in SMN levels and neuromuscular pathology were associated with a significant amelioration in the motor function and survival of SMA mice. The improvement in motor function was not simply due to increased weight or improved survival, as the mice had significantly quicker righting times by P9, well before differences in weight or survival were evident. This amelioration occurred even though mice were very weak at the start of therapy. Our results therefore provide important evidence that postsymptomatic delivery of therapeutics in SMA can be effective. This is particularly relevant for patients with SMA, as most are not diagnosed until after they display overt weakness. It remains possible that earlier intervention would be even more effective. We observed that one-quarter of SMA mice showed no response to TSA treatment. These mice tended to be more underweight compared with their littermates at P5, suggesting that their disease was more advanced and that they may have benefited from earlier treatment. It is also possible that some mice are unable to respond to TSA. Some studies in vitro have shown

variability between different patient-derived cell lines in the ability to respond to HDAC inhibitors (28). Additional study will be required to further understand the differences between responders and nonresponders. The slowed weight gain we observed in TSA-treated heterozygous and WT littermates suggests that the 10-mg/kg dose of TSA is at or near the maximum tolerated dose. Further investigation of the optimal dosing and timing of HDAC inhibition in this model system could provide invaluable insights into the treatment of the human disease.

HDAC inhibitors have been primarily developed for hematological and oncological indications (23). They have been shown to induce growth arrest, differentiation, and apoptosis in malignant cells, but nonmalignant cells are not as susceptible to the cell growth–inhibitory effects (53, 54). TSA was first isolated in 1976 as an antifungal antibiotic (55). It is a highly potent, reversible, and specific HDAC inhibitor that has not yet been developed for clinical use in part because of the prohibitive cost of isolating the compound. Recent progress has been made in the development of a process for the chemical synthesis of TSA (N. Wiech, unpublished observations), and multiple TSA analogs are also being developed (56). Other newer and more potent HDAC inhibitors are now in phase I, II, and III clinical trials and have been relatively well tolerated to date (57). A TSA-related hydroxamic acid, suberoylanilide hydroxamic acid (SAHA; also referred to as vorinostat), was recently approved by the FDA for the treatment of cutaneous T cell lymphoma. Interestingly, both TSA and SAHA appear to have relatively brief effects on histone acetylation in vivo. In humans, oral SAHA has been shown to induce a rapid increase in acetylated histones in blood within 2 hours, with a return to baseline levels by 8 hours (58). In our study, we saw transient increases in gene expression 2–6 hours after TSA dosing. This pulsatile effect on gene expression may aid the overall tolerability of HDAC inhibitors (23) and could also be more effective than constant activation at increasing the levels of specific highly regulated proteins in the cell. With repeated rounds of *SMN2* gene activation we observed increases in SMN protein of 1.5- to 2-fold, changes that are likely to be clinically meaningful, as cell lines derived from type I SMA patients have SMN protein levels approximately 40%–50% of normal (25).

SMA remains an untreatable disease, which in its most severe form is uniformly lethal. Here we have shown that the potent and specific HDAC inhibitor TSA activated *SMN2* gene expression, increased SMN protein levels, and ameliorated disease manifestations in SMA mice. These data indicate that the SMA disease phenotype can be improved even after the emergence of overt weakness, the circumstance most relevant for treatment of the human disease. Hydroxamic acids deserve further evaluation for efficacy in clinical trials in SMA patients. Consideration should also be given to combining these compounds with those that work by different mechanisms such as neuroprotection (59).

Methods

Cell culture and drug treatment. Human fibroblast cell lines from a 3-year-old type I SMA patient (GM03813; Coriell Cell Repository) with 2 copies of the *SMN2* gene, from a 7-month-old type I SMA patient (GM00232; Coriell Cell Repository) with 1 copy of the *SMN2* gene, and from a type III SMA patient (cell line no. 2906; provided by T. Crawford, Johns Hopkins University, Baltimore, Maryland, USA) with 4 copies of the *SMN2* gene were maintained as previously described (25). For drug treatments, cells were either plated in media alone or with TSA (BIOMOL International), which was dissolved in DMSO immediately before each use. The cells were then harvested for either RNA or protein isolation and quantification as previously described (25). Values were normalized to the mean of untreated cells, which was assigned as 1.

Animals and drug treatment. All experiments were carried out in accordance with the NIH Guide for the Care and Use of Laboratory Animals and were approved by the NINDS Animal Care Committee. Male FVB mice (6–8 weeks old) were purchased from Charles River Laboratories. The original breeding pairs for the SMA mice (Smn$^{+/-}$SMN2$^{+/+}$SMNΔ7$^{+/+}$) on the FVB background were provided by A. Burghes (Ohio State University, Columbus, Ohio, USA). The breeding colony was maintained by interbreeding Smn$^{+/-}$SMN2$^{+/+}$SMNΔ7$^{+/+}$ mice, and offspring were genotyped using PCR assays on tail DNA. The primers used for genotyping were 5′-CAAA-CACCTGGTATGGTCAGTC-3′ and 5′-GCACCACTGCACAACAGCCTG-3′ for the *SMN2* transgene, 5′-GCCTGCGATGTCGGTTTCTGTGAGG-3′ and 5′-CCAGCGCGGATCGGTCAGACG-3′ for the mouse knockout allele, and 5′-GTGTCTGGGCTGTAGGCATTGC-3′ and 5′-GGCTGTGCCTTTT-GGCTTATCTG-3′ for the *Smn* gene. To ensure that the *SMN2* transgene copy number did not vary with varying lifespan of the SMA pups, the ratio of the *SMN2* transgene copy number (intron 1, forward, 5′-CTC-CAGCCCTACCATGCTATG-3′; reverse, 5′-GCCAGTAGAGCAGGTTTCT-CA-3′; probe, 5′-CCCAAGACTGAACTCC-3′) to the mouse *Smn* gene copy number (MSP2 primers in the mouse promoter previously described; ref. 24) was determined by qRT-PCR of tail DNA from 4 pups with lifespans of no more than 14 days and 2 pups with lifespans of at least 25 days. This ratio was approximately 1 in all tested mice, indicating a stable *SMN2* transgene copy number of 2 in our colony.

TSA was dissolved in DMSO to a concentration of 2 or 4 μg/μl. Adult FVB animals were given 2, 5, or 10 mg/kg TSA by intraperitoneal injection in a volume of 1, 2.5, or 5 μl DMSO per gram body weight. SMA mice and their WT and heterozygous littermates received 10 mg/kg in a volume of DMSO or 2.5 μl/g body weight using a 33-gauge needle. Control animals received equal volumes of vehicle alone.

For biochemical studies, mice were anesthetized with isoflurane and then sacrificed by cervical dislocation. Brains, livers, spinal cords, and distal hind-limb skeletal muscle were dissected and flash frozen in liquid nitrogen. The tissues were stored at –80°C and thawed on ice immediately prior to RNA extraction, protein extraction, or histone extraction.

For survival studies, SMA litters were maintained and fed by the mother until P21, when they were weaned. Mice were weighed and behavioral tests were performed daily. Mice with 30% weight loss and inability to right were euthanized with carbon dioxide. Righting time was defined as the best of 2 trials of the time for the pup to turn over to its front after being placed completely on its back (maximum 30 seconds). Grip time was defined as the best of 2 trials of the time maintaining grip with the forelimbs on a bar (maximum 30 seconds).

RNA extraction and quantification. Tissue (50–100 mg) was homogenized in 1 ml TRIzol reagent (Invitrogen), and total RNA was isolated and converted to cDNA as previously described (24). Specific primers and probes were used to amplify Smn, SMN+7, and SMNΔ7 mRNA as previously described (24, 60). Primers to amplify mouse follistatin, BDNF (spliced isoform 4), ChAT, Pax7, desmin, MyoD, myogenin, embryonic MyHC, perinatal MyHC, adult MyHC-IIB, and 18S RNA were purchased from Applied Biosystems. qRT-PCR reactions were run in triplicate using the ABI Prism 7900 Sequence Detector System (Applied Biosystems). The level of each transcript was quantified by the threshold cycle (Ct) method using 18S as an endogenous control. Values were normalized to the mean of the vehicle-treated group for each tissue and gene, which was assigned as 1.

Protein extraction and semiquantitative Western blotting. Tissue samples (50–100 mg) were homogenized in 1 ml lysis buffer (0.1% NP-40 and 0.5% sodium deoxycholate) and then sonicated for 10 seconds. Total

protein concentrations were determined by the BCA Protein Assay kit (Pierce) according to the manufacturer's protocol. Protein lysates (5–10 µg for nontransgenic mice, 50–100 µg for SMA mice) were separated on 12% or 15% Tris-glycine acrylamide gels and transferred to membranes. The membranes were probed with mouse anti-SMN antibody (diluted 1:3,000; BD Transduction Laboratories) and mouse anti–α-tubulin antibody (diluted 1:10,000) or mouse anti–β-actin antibody (diluted 1:10,000; Sigma-Aldrich). Membranes containing protein lysates from nontransgenic mice were probed with the anti-mouse IgG secondary antibody labeled with IRDye800 (diluted 1:10,000; Rockland). Quantitative immunoblotting was performed as suggested by the manufacturer (Li-Cor). The membranes were scanned on an Odyssey infrared imaging system (Li-Cor), and the intensity of the protein bands was analyzed using the software provided by the manufacturer. For detection of SMN protein and actin in the SMA pups, bands were visualized with a peroxidase-linked goat anti-mouse IgG secondary antibody (diluted 1:10,000; Jackson ImmunoResearch Laboratories Inc.) and chemiluminescence detection (PerkinElmer Life Sciences). Densitometry of the resulting bands was performed using NIH Image software (http://rsb.info.nih.gov/nih-image), and SMN protein amounts were corrected for actin or tubulin values. Values were normalized to the mean of vehicle-treated mice for each tissue, which was assigned as 1.

Histones were isolated according to a protocol adapted from that of Mishra et al. (61). Briefly, 50–100 mg tissue was homogenized in 0.5 ml cold histone lysis buffer (10 mM Tris-HCl, pH 6.5, 50 mM sodium bisulfite, 1% Triton X-100, 10 mM MgCl$_2$, and 8.6% sucrose). Nuclei were isolated by centrifugation at 1,000 g for 5 minutes, washed twice with cold lysis buffer, and then washed once with cold Tris-EDTA (10 mM Tris-HCl, pH 7.4, and 13 mM EDTA). The nuclei were then resuspended in 100 µl ice-cold H$_2$O. The samples were acidified with sulfuric acid (final concentration, approximately 0.2 M), vortexed, and allowed to incubate on ice for 1 hour. The samples were then centrifuged for 10 minutes at 15,000 g. The acid-soluble proteins in the supernatant were precipitated overnight in 1 ml acetone at 25°C. The precipitated proteins were collected by centrifugation at 15,000 g for 10 minutes, and the protein pellets were allowed to air dry before being resuspended in 50–100 µl water. Protein concentrations were determined by the BCA Protein Assay kit (Pierce) according to the manufacturer's protocol. Histone proteins (2.5 µg) were separated on 16% Tris-glycine mini-gels (Invitrogen) and transferred to nitrocellulose membranes. The membranes were probed with a rabbit anti–acetylated H3 histone antibody (diluted 1:20,000; Upstate) and visualized with a peroxidase-linked goat anti-rabbit IgG secondary antibody (diluted 1:10,000; Chemicon) by chemiluminescence detection (PerkinElmer Life Sciences). The membranes were stripped and reprobed with anti–acetylated H4 histone (diluted 1:2,000; Upstate) and then anti–histone H1 (H1o/H5, diluted 1:1,000; Upstate). Densitometry of the resulting bands was performed using NIH Image software, and acetylated H3 and H4 protein amounts were corrected for H1 values. Values were normalized to the mean of vehicle-treated mice for each tissue, which was assigned as 1.

BDNF ELISA. The BDNF Emax ImmunoAssay system was used to determine BDNF protein levels according to manufacturer's instructions (Promega). Briefly, protein lysates (25 µg of brain and spinal cord, 50 µg of muscle, and 150 µg of liver) were loaded in triplicate or duplicate onto a 96-well plate precoated with monoclonal BDNF antibody to capture soluble BDNF. After washing, BDNF was detected with a polyclonal BDNF antibody and anti-IgY antibody conjugated to HRP. After incubation with a chromogenic substrate, BDNF levels were measured on a Victor^3 plate reader (PerkinElmer) and compared to a BDNF standard curve. Values were normalized to the mean of vehicle-treated samples for each tissue, which was assigned as 1.

Extract preparation and in vitro assembly of snRNPs. U1 snRNA was transcribed in vitro from a linearized template DNA in the presence of [α^{32}P]UTP (3,000 Ci/mmol) and purified from denaturing polyacrylamide gels according to standard procedures. Extracts for snRNP assembly were prepared by homogenization of frozen brain tissues in ice-cold reconstitution buffer (20 mM HEPES-KOH, pH 7.9, 50 mM KCl, 5 mM MgCl$_2$, 0.2 mM EDTA, and 5% glycerol) containing 0.01% NP-40 as previously described (38). Extracts were passed 5 times through a 25-gauge needle and centrifuged for 15 minutes at 10,500 g at 4°C. Supernatants were collected and either used directly or stored in frozen aliquots at –80°C. In vitro snRNP assembly reactions were carried out for 1 hour at 30°C in a volume of 20 µl of reconstitution buffer containing 0.01% NP-40, 25 µg whole brain extract; 10,000 cpm in vitro–transcribed, [α^{32}P]UTP-labeled U1 snRNA; 2.5 mM ATP; and 10 µM *E. coli* transfer RNA. Immunoprecipitation of snRNP assembly reactions was then carried out for 2 hours at 4°C in RSB-500 (500 mM NaCl, 10 mM Tris-HCl, pH 7.4, and 2.5 mM MgCl$_2$) containing 0.1% NP-40 and protease inhibitor cocktail (Roche) using anti-Sm Y12 (Lab Vision) antibodies bound to protein G–Sepharose. Following 5 washes with the same buffer, bound U1 snRNAs were recovered from immunoprecipitates by proteinase K treatment, phenol/chloroform extraction, and ethanol precipitation followed by electrophoresis on denaturing polyacrylamide gels and autoradiography. The amount of immunoprecipitated U1 snRNAs was quantified using a STORM 860 Phosphorimager (Molecular Dynamics) and ImageQuant software (version 4.2; Molecular Dynamics).

Pathological analysis. Mice were transcardially perfused with 4% paraformaldehyde. Lumbar spinal cords and distal hind limbs were dissected and postfixed overnight. Hind limb tissues were decalcified, embedded in paraffin, and cross-sectioned at the midpoint of the muscle. Sections (10 µm) were mounted on slides and stained with H&E. Digital images were captured using a Zeiss Axiovert 100M microscope and analyzed with NIH ImageJ software for total TA cross sectional area (original magnification, ×5), total TA myofiber number (original magnification, ×10), and myofiber diameter (original magnification, ×40). Myofiber diameter was determined by measuring the largest diameter of at least 300 neighboring myofibers per animal. Paraffin-embedded lumbar spinal cord was serially sectioned at 50-µm steps, mounted on slides, and stained with Nissl stain. Images of 15 contiguous sections, 150 µm apart (original magnification, ×10) were analyzed with NIH ImageJ software. The diameter and number of all neurons greater than 25 µm in the region below a line drawn horizontally at the level of the spinal canal were determined.

Statistics. Biochemical data were analyzed using the GraphPad Prism software package (version 3; GraphPad Software) and compared statistically by either 2-tailed Student's t test or 1-way analysis of variance followed by the Newman-Keuls multiple comparison post-hoc test. Pathological data were analyzed using STATA version 9 software. To compare differences among the 3 groups, a nonparametric equality of medians test was performed because the data were not normally distributed. If this was statistically significant, then a pairwise comparison between the 2 treatment groups was performed using a Mann-Whitney U test. $P \leq 0.05$ was considered significant.

Acknowledgments

Address correspondence to: Charlotte J. Sumner, Neurogenetics Branch, NINDS, NIH, Building 35, Room 2A1010, Bethesda, Maryland, 20892, USA. Phone: (301) 435-9288; Fax: (301) 480-3365; E-mail: sumnerc@ninds.nih.gov.

1. Pearn, J. 1978. Incidence, prevalence, and gene frequency studies of chronic childhood spinal muscular atrophy. *J. Med. Genet.* **15**:409–413.

2. Munsat, T.L., and Davies, K.E. 1992. International SMA consortium meeting. June 26–28, 1992. Bonn, Germany. *Neuromuscul. Disord.* **2**:423–428.

3. Lefebvre, S., et al. 1995. Identification and characterization of a spinal muscular atrophy-determining gene. *Cell.* **80**:155–165.

4. Frugier, T., Nicole, S., Cifuentes-Diaz, C., and Melki, J. 2002. The molecular bases of spinal muscular atrophy. *Curr. Opin. Genet. Dev.* **12**:294–298.

5. Lorson, C.L., Hahnen, E., Androphy, E.J., and Wirth, B. 1999. A single nucleotide in the SMN gene regulates splicing and is responsible for spinal muscular atrophy. *Proc. Natl. Acad. Sci. U. S. A.* **96**:6307–6311.

6. Monani, U.R., et al. 1999. A single nucleotide difference that alters splicing patterns distinguishes the SMA gene SMN1 from the copy gene SMN2. *Hum. Mol. Genet.* **8**:1177–1183.

7. Lorson, C.L., et al. 1998. SMN oligomerization defect correlates with spinal muscular atrophy severity. *Nat. Genet.* **19**:63–66.

8. Parsons, D.W., et al. 1998. Intragenic telSMN mutations: frequency, distribution, evidence of a founder effect, and modification of the spinal muscular atrophy phenotype by cenSMN copy number. *Am. J. Hum. Genet.* **63**:1712–1723.

9. Feldkotter, M., Schwarzer, V., Wirth, R., Wienker, T.F., and Wirth, B. 2002. Quantitative analyses of SMN1 and SMN2 based on real-time lightCycler PCR: fast and highly reliable carrier testing and prediction of severity of spinal muscular atrophy. *Am. J. Hum. Genet.* **70**:358–368.

10. Lefebvre, S., et al. 1997. Correlation between severity and SMN protein level in spinal muscular atrophy. *Nat. Genet.* **16**:265–269.

11. Coovert, D.D., et al. 1997. The survival motor neuron protein in spinal muscular atrophy. *Hum. Mol. Genet.* **6**:1205–1214.

12. Yong, J., Wan, L., and Dreyfuss, G. 2004. Why do cells need an assembly machine for RNA-protein complexes? *Trends Cell Biol.* **14**:226–232.

13. Wan, L., et al. 2005. The survival of motor neurons protein determines the capacity for snRNP assembly: biochemical deficiency in spinal muscular atrophy. *Mol. Cell. Biol.* **25**:5543–5551.

14. Winkler, C., et al. 2005. Reduced U snRNP assembly causes motor axon degeneration in an animal model for spinal muscular atrophy. *Genes Dev.* **19**:2320–2330.

15. Carrel, T.L., et al. 2006. Survival motor neuron function in motor axons is independent of functions required for small nuclear ribonucleoprotein biogenesis. *J. Neurosci.* **26**:11014–11022.

16. Zhang, H., et al. 2006. Multiprotein complexes of the survival of motor neuron protein SMN with Gemins traffic to neuronal processes and growth cones of motor neurons. *J. Neurosci.* **26**:8622–8632.

17. Rossoll, W., et al. 2003. Smn, the spinal muscular atrophy-determining gene product, modulates axon growth and localization of beta-actin mRNA in growth cones of motoneurons. *J. Cell Biol.* **163**:801–812.

18. Schrank, B., et al. 1997. Inactivation of the survival motor neuron gene, a candidate gene for human spinal muscular atrophy, leads to massive cell death in early mouse embryos. *Proc. Natl. Acad. Sci. U. S. A.* **94**:9920–9925.

19. Monani, U.R., et al. 2000. The human centromeric survival motor neuron gene (SMN2) rescues embryonic lethality in Smn(–/–) mice and results in a mouse with spinal muscular atrophy. *Hum. Mol. Genet.* **9**:333–339.

20. Le, T.T., et al. 2005. SMNDelta7, the major product of the centromeric survival motor neuron (SMN2) gene, extends survival in mice with spinal muscular atrophy and associates with full-length SMN. *Hum. Mol. Genet.* **14**:845–857.

21. Jarecki, J., et al. 2005. Diverse small-molecule modulators of SMN expression found by high-throughput compound screening: early leads towards a therapeutic for spinal muscular atrophy. *Hum. Mol. Genet.* **14**:2003–2018.

22. Lunn, M.R., et al. 2004. Indoprofen upregulates the survival motor neuron protein through a cyclooxygenase-independent mechanism. *Chem. Biol.* **11**:1489–1493.

23. Minucci, S., and Pelicci, P.G. 2006. Histone deacetylase inhibitors and the promise of epigenetic (and more) treatments for cancer. *Nat. Rev. Cancer.* **6**:38–51.

24. Kernochan, L.E., et al. 2005. The role of histone acetylation in SMN gene expression. *Hum. Mol. Genet.* **14**:1171–1182.

25. Sumner, C.J., et al. 2003. Valproic acid increases SMN levels in spinal muscular atrophy patient cells. *Ann. Neurol.* **54**:647–654.

26. Brichta, L., et al. 2003. Valproic acid increases the SMN2 protein level: a well-known drug as a potential therapy for spinal muscular atrophy. *Hum. Mol. Genet.* **12**:2481–2489.

27. Chang, J.G., et al. 2001. Treatment of spinal muscular atrophy by sodium butyrate. *Proc. Natl. Acad. Sci. U. S. A.* **98**:9808–9813.

28. Andreassi, C., et al. 2004. Phenylbutyrate increases SMN expression in vitro: relevance for treatment of spinal muscular atrophy. *Eur. J. Hum. Genet.* **12**:59–65.

29. Hirtz, D., et al. 2005. Challenges and opportunities in clinical trials for spinal muscular atrophy. *Neurology.* **65**:1352–1357.

30. Sumner, C.J. 2006. Therapeutics development for spinal muscular atrophy. *NeuroRx.* **3**:235–245.

31. Sanderson, L., et al. 2004. Plasma pharmacokinetics and metabolism of the histone deacetylase inhibitor trichostatin A after intraperitoneal administration to mice. *Drug. Metab. Dispos.* **32**:1132–1138.

32. Korzus, E., Rosenfeld, M.G., and Mayford, M. 2004. CBP histone acetyltransferase activity is a critical component of memory consolidation. *Neuron.* **42**:961–972.

33. Camelo, S., et al. 2005. Transcriptional therapy with the histone deacetylase inhibitor trichostatin A ameliorates experimental autoimmune encephalomyelitis. *J. Neuroimmunol.* **164**:10–21.

34. Iezzi, S., et al. 2004. Deacetylase inhibitors increase muscle cell size by promoting myoblast recruitment and fusion through induction of follistatin. *Dev. Cell.* **6**:673–684.

35. Castro, L.M., Gallant, M., and Niles, L.P. 2005. Novel targets for valproic acid: up-regulation of melatonin receptors and neurotrophic factors in C6 glioma cells. *J. Neurochem.* **95**:1227–1236.

36. Minetti, G.C., et al. 2006. Functional and mor-

phological recovery of dystrophic muscles in mice treated with deacetylase inhibitors. *Nat. Med.* **12**:1147–1150.

37. Pellizzoni, L., Yong, J., and Dreyfuss, G. 2002. Essential role for the SMN complex in the specificity of snRNP assembly. *Science.* **298**:1775–1779.

38. Gabanella, F., Carissimi, C., Usiello, A., and Pellizzoni, L. 2005. The activity of the spinal muscular atrophy protein is regulated during development and cellular differentiation. *Hum. Mol. Genet.* **14**:3629–3642.

39. Wooten, G.F., Park, D.H., Joh, T.H., and Reis, D.J. 1978. Immunochemical demonstration of reversible reduction in choline acetyltransferase concentration in rat hypoglossal nucleus after hypoglossal nerve transection. *Nature.* **275**:324–325.

40. Terenghi, G. 1999. Peripheral nerve regeneration and neurotrophic factors. *J. Anat.* **194**:1–14.

41. Glass, D.J. 2003. Signalling pathways that mediate skeletal muscle hypertrophy and atrophy. *Nat. Cell Biol.* **5**:87–90.

42. Cossu, G., and Biressi, S. 2005. Satellite cells, myoblasts and other occasional myogenic progenitors: possible origin, phenotypic features and role in muscle regeneration. *Semin. Cell Dev. Biol.* **16**:623–631.

43. Fidzianska, A., Goebel, H.H., and Warlo, I. 1990. Acute infantile spinal muscular atrophy: muscle apoptosis as a proposed pathogenetic mechanism. *Brain.* **113**:433–445.

44. Soubrouillard, C., et al. 1995. Expression of developmentally regulated cytoskeleton and cell surface proteins in childhood spinal muscular atrophies. *J. Neurol. Sci.* **133**:155–163.

45. Wharton, S., and Ince, P.G. 2003. Pathology of motor neuron disorders. In *Motor Neuron Disorders.* P.J. Shaw and M.J. Strong, editors. Butterworth Heinemann. Philadelphia, Pennsylvania, USA. 17–49.

46. Arnold, A.S., et al. 2004. Reduced expression of nicotinic AChRs in myotubes from spinal muscular atrophy I patients. *Lab. Invest.* **84**:1271–1278.

47. Shafey, D., Cote, P.D., and Kothary, R. 2005. Hypomorphic Smn knockdown C2C12 myoblasts reveal intrinsic defects in myoblast fusion and myotube morphology. *Exp. Cell Res.* **311**:49–61.

48. Braun, S., Croizat, B., Lagrange, M.C., Warter, J.M., and Poindron, P. 1995. Constitutive muscular abnormalities in culture in spinal muscular atrophy. *Lancet.* **345**:694–695.

49. Chan, Y.B., et al. 2003. Neuromuscular defects in a Drosophila survival motor neuron gene mutant. *Hum. Mol. Genet.* **12**:1367–1376.

50. Tissenbaum, H.A., and Parry, D.J. 1991. The effect of partial denervation of tibialis anterior (TA) muscle on the number and sizes of motorneurons in TA motornucleus of normal and dystrophic (C57BL dy2j/dy2j) mice. *Can. J. Physiol. Pharmacol.* **69**:1769–1773.

51. Funakoshi, H., et al. 1995. Muscle-derived neurotrophin-4 as an activity-dependent trophic signal for adult motor neurons. *Science.* **268**:1495–1499.

52. Gui, C.Y., Ngo, L., Xu, W.S., Richon, V.M., and Marks, P.A. 2004. Histone deacetylase (HDAC) inhibitor activation of p21WAF1 involves changes in promoter-associated proteins, including HDAC1. *Proc. Natl. Acad. Sci. U. S. A.* **101**:1241–1246.

53. Warrener, R., et al. 2003. Tumor cell-selective

cytotoxicity by targeting cell cycle checkpoints. *FASEB J.* **17**:1550–1552.

54. Ungerstedt, J.S., et al. 2005. Role of thioredoxin in the response of normal and transformed cells to histone deacetylase inhibitors. *Proc. Natl. Acad. Sci. U. S. A.* **102**:673–678.

55. Tsuji, N., Kobayashi, M., Nagashima, K., Wakisaka, Y., and Koizumi, K. 1976. A new antifungal antibiotic, trichostatin. *J. Antibiot. (Tokyo).* **29**:1–6.

56. Moradei, O., Maroun, C.R., Paquin, I., and Vaisburg, A. 2005. Histone deacetylase inhibitors: latest developments, trends and prospects. *Curr. Med. Chem. Anticancer Agents.* **5**:529–560.

57. Marks, P.A., and Dokmanovic, M. 2005. Histone deacetylase inhibitors: discovery and development as anticancer agents. *Expert Opin. Investig. Drugs.* **14**:1497–1511.

58. O'Connor, O.A., et al. 2006. Clinical experience with intravenous and oral formulations of the novel histone deacetylase inhibitor suberoylanilide hydroxamic acid in patients with advanced hematologic malignancies. *J. Clin. Oncol.* **24**:166–173.

59. Haddad, H., et al. 2003. Riluzole attenuates spinal muscular atrophy disease progression in a mouse model. *Muscle Nerve.* **28**:432–437.

60. Sumner, C.J., et al. 2006. SMN mRNA and protein levels in peripheral blood: biomarkers for SMA clinical trials. *Neurology.* **66**:1067–1073.

61. Mishra, N., Reilly, C.M., Brown, D.R., Ruiz, P., and Gilkeson, G.S. 2003. Histone deacetylase inhibitors modulate renal disease in the MRL-lpr/lpr mouse. *J. Clin. Invest.* **111**:539–552. doi:10.1172/JCI200316153.